Journal of Hydrology: Regional Studies 34 (2021) 100797

Contents lists available at ScienceDirect

Journal of Hydrology: Regional Studies

journal homepage: www.elsevier.com/locate/ejrh

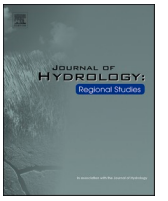

Towards climate-adaptive development of small hydropower projects in Himalaya: A multi-model assessment in upper Beas basin

Tejal S. Shirsat [a,*], Anil V. Kulkarni [a], Andrea Momblanch [b], S.S. Randhawa [c], Ian P. Holman [b]

[a] Divecha Centre for Climate Change, Indian Institute of Science, 560012, Bangalore, India
[b] Cranfield University, College Road, MK43 0AL, Cranfield, Bedfordshire, United Kingdom
[c] Himachal Pradesh Council for Science Technology and Environment, 171001, Shimla, India

ARTICLE INFO

Keywords:
Glaciers
Indus
Snowmelt
Climate change
Modelling
WEAP

ABSTRACT

Study Region: Allain catchment, a sub-basin of Beas basin, Western Himalaya.
Study Focus: This study aims to assess future glacio-hydrological changes in a small basin and their impacts on the operation of two Small Hydropower Projects (SHP) with contrasting hydrological requirements. The Water Evaluation and Planning (WEAP) model is used to integrate cryosphere, hydrology and hydropower production modelling in the 21st century using climate changes projected by the ensembles of five global climate models under RCP 4.5 and 8.5.
New Hydrological Insights for the Region: The total streamflow in the future is projected to have widespread uncertainty in the magnitude but shows noticeable changes in the seasonality. Of the two SHPs, the one utilizing high flows with low hydraulic head shows a power generation behaviour similar to streamflow projections. Its annual hydropower production is projected to change by 2 to 21% (RCP4.5) and -5 to 40% (RCP8.5) by the end of the century. The other plant that uses lesser flows but high head maintains its designed power production consistently throughout the century. The study indicates that the design of hydropower plants strongly influences their sensitivity to future climate and thus provides important insights into the climate-adaptive designs and planning of future hydropower projects in Himalaya.

1. Introduction

The Hindukush- Karakoram-Himalayan (HKH) region is often referred to as "Water Towers of Asia" due to its large concentration of glaciers and seasonal snow that sustains yearlong water supply of major rivers such as Indus, Ganga and Brahmaputra. About 800 million people living in the mountains and downstream region rely on the water originating in the HKH region for agriculture, hydropower generation, industrial and domestic usage (Immerzeel et al., 2020; Pritchard, 2019). These rivers are sustained by snow and glacier melt, rainfall and groundwater, although the contribution of individual components varies spatially between the sub-basins and temporally between the seasons, giving this region a complex hydrological nature (Lutz et al., 2014).

Owing to the steep topographical gradient and the perennial water supply, the HKH region has a large hydropower generation

* Corresponding author.
E-mail addresses: shirsat.tejal@gmail.com, shirsats@iisc.ac.in (T.S. Shirsat).

https://doi.org/10.1016/j.ejrh.2021.100797
Received 17 October 2020; Received in revised form 12 February 2021; Accepted 17 February 2021
Available online 11 March 2021

potential. The gross hydropower potential of the Indian HKH region is around 117 gigawatt (GW); most of which is potentially suitable for large hydropower projects (i.e. with a capacity greater than 25 megawatt (MW)) (CEA, 2020). However, large hydropower plants usually require storage structures which are difficult and expensive to realize due to the rugged terrain and incompatible with existing water-sharing treaties in the region (Hussain et al., 2019). In contrast, SHPs with 2–25 MW capacity of the run-of-river type have lower costs related to the necessary built infrastructure and have fewer adverse effects on the environment and local communities (Kumar and Katoch, 2014). At present, out of the cumulative feasible SHP potential of 8.5 GW in the Indian HKH region, only 1.6 GW have been installed, some under the United Nations' Clean Development Mechanism (CDM) (NEP, 2018). Therefore, a major part of the SHP potential in India is yet to be tapped. Consequently, the Ministry of New Renewable Energy of India is extensively promoting the development of SHP with a target to expand the installed capacity to 5 GW by 2022 (NEP, 2018). Both government and private sectors are actively investing in the increasing small hydropower facilities in the Himalayas. Thus, information about the changing future water availability and its interaction with plant design (e.g. discharge and head requirements) is critical to ensure the long-term suitability of infrastructure and investments.

The hydrology of the HKH rivers is influenced by the precipitation regime, snow and glacier melt in the summer and the characteristics of glaciers. However, the recent changes in the climatic conditions have had critical impacts on the state of cryospheric resources. In most regions of the Himalayas, glaciers are retreating, thinning and losing mass (Azam et al., 2018; Bolch et al., 2012). Glacier mass balance observations suggest an increase in mass wastage in the last decade (Maurer et al., 2019; Mukherjee et al., 2018; Tawde et al., 2017) with small and low-altitude glaciers losing mass at a higher rate than large glaciers (Prasad et al., 2019; Tawde et al., 2017). Also, monitoring of winter precipitation in the Western Himalaya suggests an increase in total precipitation but a decrease in snowfall from 1991 to 2015 (Negi et al., 2018). These changes in the cryosphere will alter the spatial pattern and timing of glacier and snow melt (Immerzeel et al., 2012; Lutz et al., 2014), which may have a profound impact on the amount and seasonality of water available for hydropower generation.

Most of the river runoff modelling studies in Himalaya focus on large basins covering areas larger than 5000 km^2 (Momblanch et al., 2019a); however, the decision making regarding the small hydropower sector occurs at small watersheds. Several studies have explored the hydrological regimes of small Himalayan watersheds using a range of modelling approaches from detailed glacio-hydrological models (Immerzeel et al., 2012; Ragettli et al., 2015) to simple empirical relationships between temperature and melt (Azam et al., 2019; Kulkarni et al., 2002; Rathore et al., 2011). The former methods require large amounts of data at a high spatio-temporal resolution which are often not available in high elevation catchments, whereas the simplicity of the later methods inhibits them from taking the complex water demand structures into account. Consequently, conceptual models, which integrate the

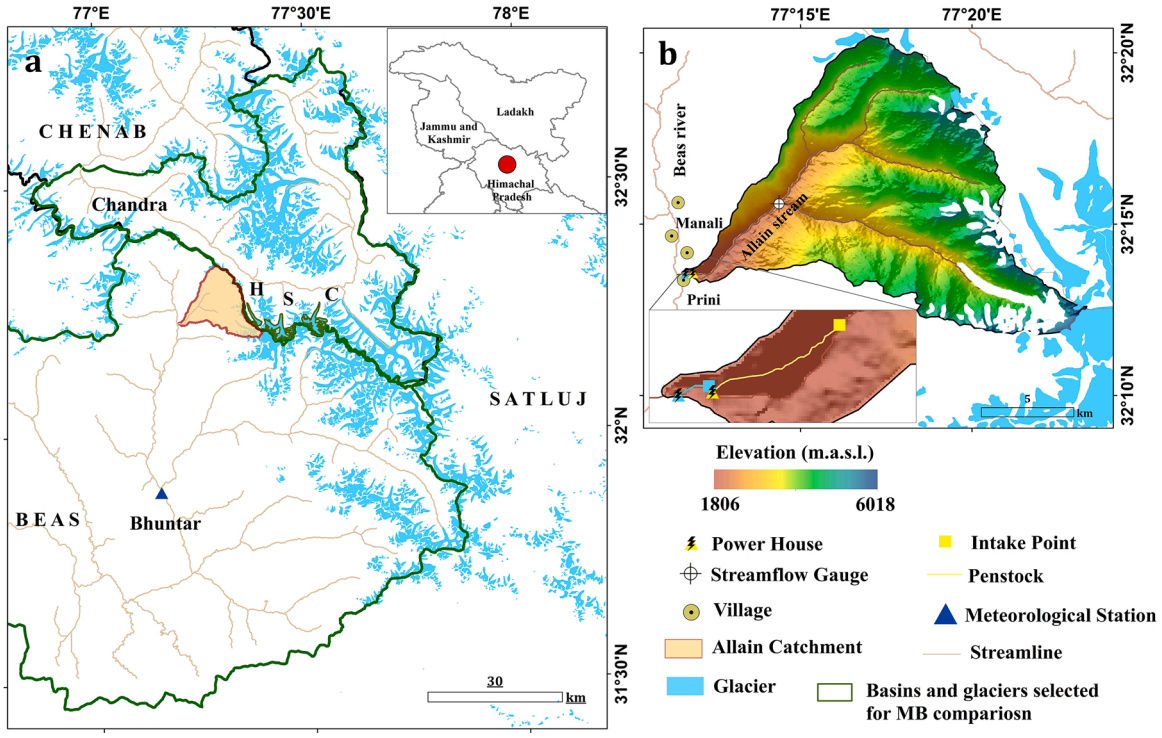

Fig. 1. Location map of the study area. Panel a shows location of Allain catchment in Beas basin along with the meteorological station Bhuntar. Additional basins (Beas and Chandra) and individual glaciers (Hamtah, Sakchum and Chhota Shigri denoted as H, S and C, respectively) selected for comparative mass balance estimates are located adjacent to Allain catchment (Table S1). Panel b shows Allain catchment on ASTER DEM along with locations of the streamflow gauge and nearby towns of Manali and Prini. The inside box shows the close-up of the powerhouses of Aleo-1 (Yellow) and Aleo-2 (Blue) plants with intake points and penstocks.

main hydrological processes with water uses and infrastructures and simulate energy production in multiple hydropower plants over time in a single run, offer an appropriate alternative (Momblanch et al., 2019b).

The present study aims to assess the future changes in hydropower generation of two SHP with contrasting discharge-head designs and discuss the implications for future SHP design in the HKH. We have used a water resource systems model that integrates cryospheric resources, hydrological processes, water infrastructures and water demands. We conduct a robust evaluation of the historical model performance using glacier Mass Balance (MB), MODIS Snow Cover Area (SCA) and measured discharge. Then, future changes in runoff and hydropower generation are estimated until the end of the century considering the projections of two ensembles of five global climate models (GCM) representing different types of future climates under Representative Concentration Pathway (RCP) 4.5 and 8.5.

2. Study area and data

The two selected run-of-river power projects *viz*., 3 MW Aleo Manali and 4.8 MW Aleo-2 hydropower projects (henceforth called as Aleo-1 and Aleo-2, respectively) are situated on the Allain stream near Manali in the state of Himachal Pradesh in India (Fig. 1) (Table 1). The Allain stream is a tributary of the Beas river which is a part of the Indus river system. The catchment area of the power project is 140.2 km^2 with an altitudinal range from 1806 to 6018 m. a. s. l. Around 47% of the catchment area is covered by grassland, with 22 and 23% of forest and barren land cover, respectively. A small agricultural area, located at the tip of the catchment near the village of Prini, accounts for just 0.3% of the total catchment area. The mean annual SCA in the catchment is 64%. There are 22 glaciers in the catchment covering an area of 10.9 km^2. The average glacier area is 0.5 km^2, and the glaciers cover the altitudinal range from 3672 to 5488 m.a.s.l.

The catchment is located in the monsoon-arid transition zone and is influenced by western disturbances from November to April and the Indian summer monsoon from May to October (Azam et al., 2019). Mean annual precipitation recorded at the Bhuntar meteorological observatory (Fig. 1) is 975 mm with equal contributions from both western disturbances and the Indian monsoon. The mean annual temperature is 17.8 °C and ranges from 8.9 °C to 25.6 °C. The major seasons in the study area are considered as autumn (October-November), winter (December- March), summer (April- June) and monsoon (July- September) (Kulkarni et al., 2002).

The meteorological, land cover, soil and glacier data used in this study were acquired from satellite and *in-situ* observations. Temperature and precipitation data from 1984 to 2018 were acquired from the Bhuntar meteorological observatory (1092 m. a. s. l.), situated 37 km from the catchment. The data was extrapolated to different elevation bands using a linear temperature lapse rate of -6.5 °C/km and a Beas-specific precipitation gradient of 0.04%/m (Prasad et al., 2019). Discharge measurements from July 2010 to February 2018 were collected from the Allain Duhangan Hydropower Plant (ADHPL) at the Allain Barrage in the catchment. The details of the satellite datasets used are presented in Table 2. In addition, the Volume-Area (V-A) scaling parameters are taken from Prasad et al. (2019).

Temperature and precipitation outputs of five GCMs *viz*., INMCM4, MIROC5, IPSL-CM5A-LR, GFDL-CM3 and CanESM2 of Coupled Model Intercomparison Project Phase 5 (CMIP5) (Taylor et al., 2012) that project different possible future climates by the end of the century under RCP4.5 and 8.5 are used in the present study (Table 3). Li et al. (2019) utilized these models in Beas basin and reported a broad spread of future river discharge resulting from the range of future temperatures and precipitation projections. Thus, the selected climate models are helpful to understand the response of hydrological variables and hydropower plants to a variety of climate change scenarios as well as to cover the large uncertainty space in future runoff modelling.

3. Methods

3.1. Model setup

WEAP is a conceptual, semi-distributed model for the analysis of water resource systems taking different water resources (rainfall, snow and glacier melt) and water demands (hydropower) into account (Sieber and Purkey, 2015). The catchment is divided into 100 m elevation bands, and each elevation band is considered as an individual hydrological element with up to four land cover classes (i.e. agriculture, forest, grassland and barren land). Glaciers in each elevation band are considered as separate hydrological elements to ensure that the model captures glacier evolution accurately (Momblanch et al., 2019b). We use WEAP's soil moisture method as it takes snow and glacier melt and glacier evolution into account in the runoff modelling. This method is based on a two-compartment

Table 1
Details of the Aleo-1 and Aleo-2 small hydropower projects.

Characteristic	Aleo-1	Aleo-2
Installed Capacity (MW)	3	4.8
Units	2 units of 1.5 MW	2 units of 2.4 MW
Elevation of Powerhouse (m. a. s. l.)	1861	1820
Hydraulic Head (m)	290.4	36.3
Design Discharge (m^3/s)	1.33	15.8
Turbine type	Pelton	Francis
Generating Efficiency	80%	80%
Date of Commissioning	August, 2005	January, 2014

Table 2
Details of satellite datasets used in the study.

Dataset	Spatial/ Temporal Resolution	Time period	Purpose	Source
ASTER DEM	30*30m	2011	Delineation of catchment boundary and elevation bands	earthexplorer.usgs.gov
Global Land Cover 30	30*30m	2000	Identification of land use classes	globallandcover.com
Harmonized World Soil database (version 1.2)	1*1 km	2012	Identification of soil types	fao.org
NASA SSE Relative Humidity at 2 m (release 6.0)	0.5*0.5°/ Monthly	1984–2018	Evapotranspiration calculation	asdc-arcgis.larc.nasa.gov/sse
NASA SSE Wind Speed at 2 m (release 6.0)	0.5*0.5°/ Monthly	1984–2018	Evapotranspiration calculation	asdc-arcgis.larc.nasa.gov/sse
MODIS Snow Cover Area MOD10A2	500*500 m/ 8 days	2004–2016	Snow Cover extraction	earthdata.nasa.gov
INSAT- 3D Cloud Mask	4 km* 4 km/ 30 minutes	2013–2018	Estimation of Cloudiness Fraction	mosdac.gov.in
Randolph Glacier Inventory (version 6.0)	Not applicable	2002	Glacier outlines	glims.org

Table 3
Details of the climate projections used in the study. ΔT and ΔP denote to absolute change in mean annual temperature and relative change in annual precipitation compared to the baseline by the end of the century.

	GCM	Spatial Resolution ()	RCP	ΔT (°C)	ΔP (%)	Description
1	INMCM4	1.5 × 2	4.5	1.6	−3.7	Cold and Dry
2			8.5	4.2	13.8	Cold and Wet
3	MIROC5	1.9 × 3.8	4.5	2.5	23.1	Cold and Wet
4			8.5	4.4	34.9	Cold and Wet
5	IPSL-CM5A-LR	1.9 × 3.8	4.5	3.8	17.9	Warm and Wet
6			8.5	7.6	−10.3	Warm and Dry
7	GFDL-CM3	2 × 2.5	4.5	3.7	−4.1	Warm and Dry
8			8.5	5.9	2.6	Warm and Dry
9	CanESM2	2.8 × 2.8	4.5	3.2	16.4	Warm and Wet
10			8.5	6.1	56.3	Warm and Wet

Note that the descriptions cold/warm and dry/wet indicate the relative differences in temperature and precipitation changes among the future projections. Warm scenarios show higher temperature increase compared to cold scenarios and wet scenarios have larger increase in precipitation compared to dry scenarios.

soil water balance that describes evapotranspiration, surface runoff, interflow and baseflow for a watershed (Sieber and Purkey, 2015). Evapotranspiration is calculated using a simplified Penman-Monteith equation (Yates et al., 2005) in the upper compartment along with surface runoff and interflow, whereas baseflow is estimated in the lower compartment. Soil properties such as soil storage capacity, hydraulic conductivity, preferred flow direction and runoff resistance factor are allocated to each land cover area within an elevation band and are calibrated later (Yates et al., 2005).

The model is set up from October 1983 to February 2018 with a monthly time step. The two years from October 1983 to September 1985 were used as a warm-up period to remove the effect of initial conditions. Due to the small population and agricultural areas, we assume that the human water demand in the catchment other than for hydropower is negligible and thus use only the hydrological and power generation modelling capacities of WEAP.

3.2. Model calibration and validation

We adopt a three-fold calibration technique to ensure the model captures the present glacier condition, snow cover area and streamflow realistically. First, we manually calibrated the snow freezing and melting points and the ice melting point in the glaciated catchment by comparing the aggregate glacier mass balance in WEAP against the mass balance estimated from the Improved Accumulation Area Ratio (IAAR) Method (Tawde et al., 2017) for 22 glaciers in the catchment. The glacier mass balance estimates from 1986-2000 were used for calibration and 2001–2011 for validation. Secondly, we manually calibrated the snow freezing and melting points for non-glaciated catchments through the comparison of the simulated areas covered by snow in WEAP and MODIS SCA. Due to MODIS SCA data availability, the time period of 2004–2010 was used for calibration, whereas 2011–2016 was used for validation. Lastly, the soil parameters for each land cover class were calibrated using the Parameter Estimation Tool (PEST) against the measured discharge. Here, the time period 2010–2014 was used for calibration and 2015–2018 was for validation. WEAP, as a conceptual model, relies on the calibration process and such a thorough stepwise calibration approach helps in minimising internal inconsistency and reduces the risk of error compensation (Ragettli et al., 2014).

3.3. MODIS snow cover extraction

MODIS Terra 8 days maximum snow cover product (MOD10A2) images were extracted to the spatial boundaries of each elevation band to obtain SCA. Images with more than 10% cloud cover were eliminated from the time series (Tahir et al., 2015), which accounted for 6% of the total images. Cloud pixels were corrected as no-snow or snow pixels based on the surrounding pixels from the remaining images based on the critaria described in Muhammad and Thapa (2020) by visual interpretation, taking special care in winter images. This approach helps in effectively removing cloud pixels and providing reliable estimates of SCA in the catchment. Finally, the average monthly mean SCA was estimated by taking the average of the (up to) four images available in a month.

3.4. Future projections of climate variables and glacier area

The outputs of the selected climate models were extracted from 1986 until the end of the century for the grid location of Bhuntar station as the model is calibrated for present using the in-situ data measured at the same station (Tawde et al., 2019). Later, the change factor method (Anandhi et al., 2011) was used to bias correct the monthly means of temperature and precipitation projections for 20-year time slices throughout the century, taking 1986–2005 as the baseline period. These data were used to calculate additive and multiplicative monthly mean change factors for temperature and precipitation, respectively, for 2050 (average of 2041–2060) and 2090 (average of 2081–2100), which were applied to the base data at Bhuntar station. Future changes in glacier area were estimated using a glacier geometry model based on V-A scaling (Marzeion et al., 2012) and the future climate projections for each time slice (Prasad et al., 2019); a detailed description of this methodology can be found in the publications mentioned above. Finally, WEAP was forced with the future temperature, precipitation and glacier areas to simulate stream runoff and hydropower generation until the end

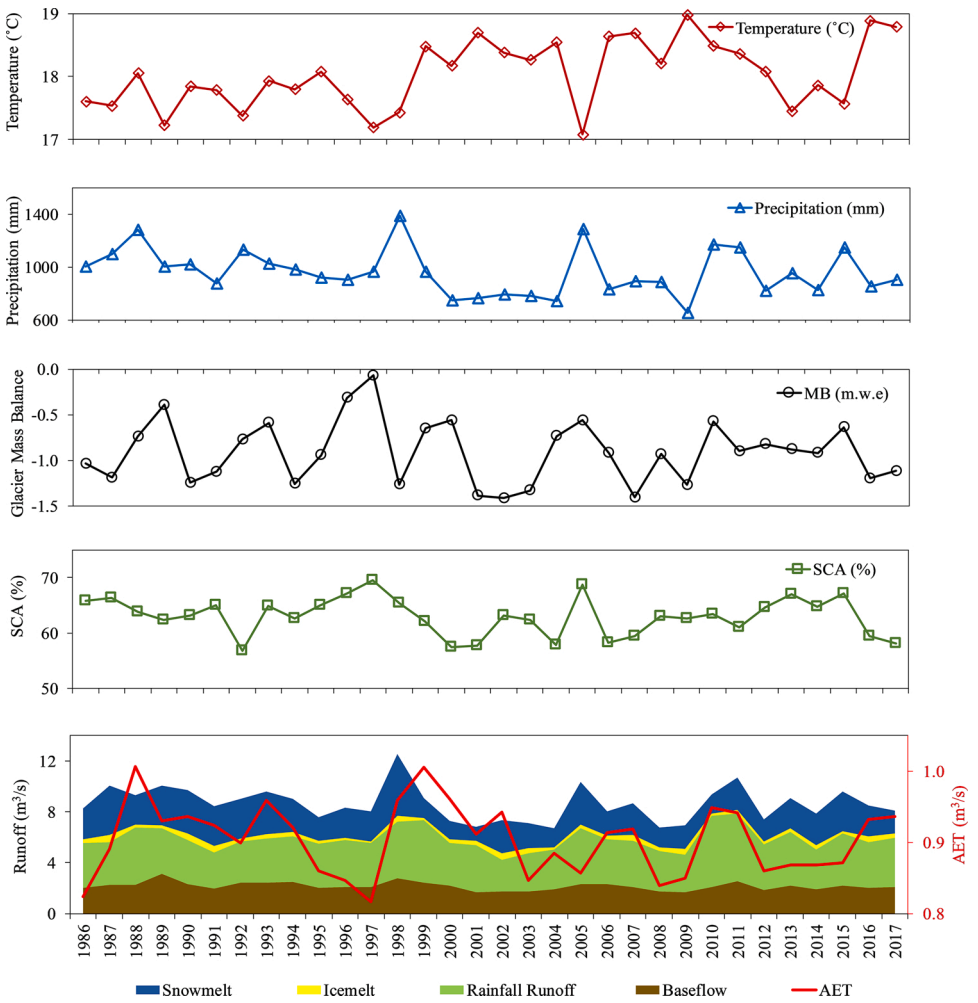

Fig. 2. Interannual variation in the streamflow contributions and actual evapotranspiration (AET) (m^3/s) at the catchment outlet, mean simulated SCA (% of the total catchment area) and glacier MB (m.w.e.) in the catchment, and mean annual temperature and precipitation observed at Bhuntar observatory.

of the century. Future power generation was simulated at both plants, assuming that there will not be new water resources developments in the Allain river in the future.

4. Results

4.1. Model calibration and validation

The total mass loss of 22 glaciers in the catchment simulated by WEAP during the calibration and validation periods is -12.2 and -11.4 meter water equivalent (m.w.e.), respectively, compared to -12.3 and -11.3 m.w.e. by the IAAR method. Our annual and cumulative MBs are in unison with the IAAR method (Fig. S1). Furthermore, a comparison of our average annual mass balance estimates in the Allain catchment with previous studies in the surrounding area at glacier or basin scale shows good agreement (Table S1).

Results of the calibration and validation with MODIS SCA show that WEAP is able to reproduce SCA adequately in the catchment (Fig. S2), with R^2 of 0.79 and 0.73, respectively. The maximum SCA in winter and minimum SCA simulated in monsoon agree well with MODIS SCA, although the SCA in summer is underestimated by WEAP whereas autumn SCA is overestimated. This can be attributed to the linear temperature and precipitation gradient due to which WEAP starts building SCA earlier than actual snowfall in the catchment. The lack of snow redistribution in WEAP could also contribute to the underestimation of summer SCA (Ragettli et al., 2014).

Calibration and validation against the measured river discharge show that model performance (Fig. S3 and Table S3) is excellent for Nash-Sutcliffe Efficiency (NSE) (0.89 and 0.83) and Percent Bias (PBIAS) (-0.31% and -1.13%) for calibration and validation, respectively, according to the monthly flow performance criteria of Moriasi et al. (2007). We observe that the model can reproduce low winter flows accurately but tends to underestimate the monsoon flows, which leads to a small negative bias. This tendency was also observed in other modelling studies in the Beas basin by Li et al. (2019) and Momblanch et al. (2019b). Overall, considering the limitations and uncertainty of hydrological modelling in complex mountainous regions, the WEAP model performs well in reproducing the present cryosphere and hydrology of the study area. Further details of the calibration and validation can be found in the supplementary material.

4.2. Hydrological regime

Analysis of the simulated hydrological components suggests that the annual streamflow is mostly contributed by rainfall-runoff (43%), snowmelt (28.3%) and baseflow (25%) with a small contribution from glacier melt (3.8%) during 1986–2017. However, the contributions vary from year to year, as shown in Fig. 2. A relatively high baseflow proportion is consistent with observations that baseflow in the area is enhanced by winter-spring snowmelt infiltration to groundwater (Maurya et al., 2018). High flow peaks of 1998 and 2005 are associated with increased winter precipitation. In contrast, the peak of 2011 was caused by increased monsoon precipitation as seen by the increase in snowmelt and rainfall runoff contributions, respectively. The low flow years such as 2000–2002 are associated with a higher simulated contribution (up to 7% of annual flow) of glacier melt, demonstrating the tendency of glacier melt to have a buffering effect in drought years in the Indus basin (Pritchard, 2019).

4.3. Hydropower generation

Hydropower generation was calculated at both Aleo-1 and Aleo-2 power projects using the simulated runoff and the relevant plant details. Simulated power generation of the Aleo-1 power project (Fig. 3) is consistent throughout the year as its higher head and low flow requirement are always satisfied by the streamflow. In contrast, the higher flow requirement of the Aleo-2 power project are not fulfilled by the stream yearlong leading to monthly variations in the power generation (Fig. 3) similar to streamflow, with maximum power generated in July when the plant runs at full capacity and minimum hydropower generated in February when streamflow is

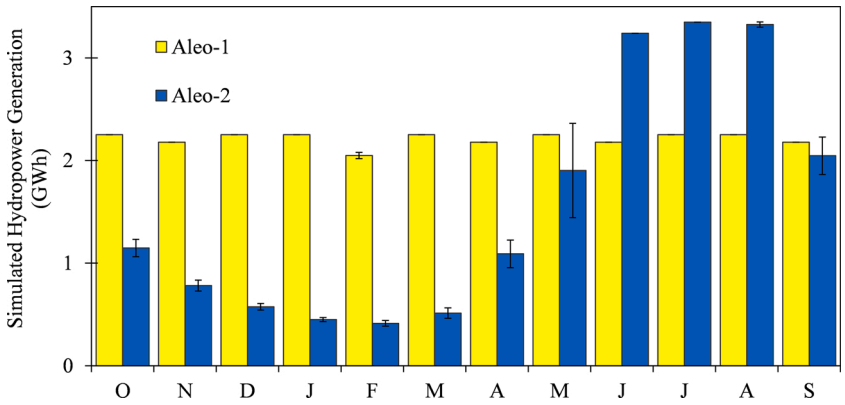

Fig. 3. Simulated average monthly hydropower generation (GWh) at Aleo-1 and Aleo-2 Hydropower projects. Average for Aleo-1 is from 2005-2018 whereas for Aleo-2 is taken from 2014-2018 based on the start of the operation of the projects. Error bars indicate the inter-annual variation.

generally lowest. These different design criteria lead to the average annual hydropower generation at Aleo-1 and Aleo-2 projects of 26.5 and 18.8 Gigawatt-hour (GWh) being 100% and 45% of their total annual generation potential given their installed capacity of 3 MW and 4.8 MW, respectively.

4.4. Future projections

The climate change scenarios used in the study suggest a consistent increase in the mean annual temperature throughout the century compared to the base period, whereas the changes in precipitation show large variation within the models. The WEAP model outputs show a significant sensitivity of the studied system to these varied future climate change scenarios. SCA was simulated to steadily reduce through the century along with the glacier extent in all the scenarios. The total discharge of Allain stream shows considerable uncertainty in the magnitude and direction of change between the individual ensemble members but a prominent change in the seasonality. The projected changes in significant elements of study are summarised in Table 4 and are elaborated in the subsequent sections.

4.4.1. Future climate change

The mean annual temperature projected to increase by 3 °C (RCP4.5) and 5.6 °C (RCP8.5) by the end of the century where the cold scenarios show less warming compared to warm scenarios. INMCM4 projects the least warming whereas IPSL-CM5A-LR shows the highest warming by the end of the century in both RCP 4.5 and 8.5 scenarios. The precipitation by the end of the century may increase by 9.9% (RCP4.5) and 19.5% (RCP8.5), with large spread within the models. CanESM2 projects increases in the winter precipitation whilst MIROC5 shows strengthening of monsoon precipitation by the end of the century (Fig. 4). WEAP results suggest that the proportion of snowfall in total precipitation will decline gradually from 59.6% in the baseline to 48.3% (RCP4.5) and 45% (RCP8.5) by 2050; it will further reduce to 41.6% (RCP4.5) and 33.7% (RCP8.5) by 2090.

4.4.2. Future changes in cryosphere

The entire area of the small and low altitude glaciers in the catchment is below the equilibrium line altitude in all the climate change scenarios used in the study which drives their rapid retreat in future. They are projected to lose about 83–86% of the mass by 2050 and disappear completely by the end of century. The mass loss is rapid till the middle of the century, decreasing from 0.41 Gt in 2000 to about 0.07 Gt in 2050, but slows down by the end of century (Tawde et al., 2019). The annual glacier mass balance gradually decreases from -0.88 m.w.e. in 2000 to -1.39 m.w.e. in RCP4.5 and -1.45 in RCP8.5 up to 2050.

Projected SCA was also observed to decrease continuously until the end of century as increased temperatures lead to a higher proportion of precipitation falling as rain (Fig. 5). Maximum SCA depletion occurs in August in the baseline scenario while it is simulated to advance to May-June in 2090 as result of earlier snow melt. Average SCA in the catchment declines by 15.3% (RCP4.5) and 34.8% (RCP8.5) by the end of century. The winter SCA of 98% of the catchment area in the baseline reduces to 94% (RCP4.5) and 84.6% (RCP8.5) in 2090. Overall, the warmer and drier climate projected by IPSL-CM5A-LR in RCP8.5 projects the highest loss in the cryospheric components whereas CanESM2 in which winter precipitation increases significantly, shows the least reduction in cryosphere.

4.4.3. Future hydrological change

Rising temperature and liquid precipitation in the future result in AET being projected to increase continuously throughout the century by 30.7% (RCP4.5) and by 52.7% (RCP8.5) in 2090. The simulated streamflow shows variation based on the forcing of each climate change scenario; it is projected decrease in the cold-dry and warm-dry forcings, whereas it increases in the wet scenarios. The average annual streamflow is projected to change by -12 to 14.6% (RCP4.5) and by -18.6–48.1% (RCP8.5) by 2090.

Changes in the cryospheric components in the catchment result in the changes in the contributions of different hydrologic components (snowmelt, icemelt, rainfall-runoff and baseflow). Snow and glacier melt runoff contribution in the total streamflow is observed to gradually decrease in all climate change scenarios, whereas rainfall runoff contribution increases by the end of century (Table 5). Baseflow is also observed to increase gradually till the end of century contributing about 29% of total annual streamflow

Table 4
The projected changes in the major hydrological and cryospheric components and hydropower production by 2050 and 2090 compared to the base period; the values are the ensemble means of 5 GCM outputs and the values in bracket indicate (minimum/maximum) values.

	2050 RCP4.5	2050 RCP8.5	2090 RCP4.5	2090 RCP8.5
ΔT (°C)	2 (1.2/2.9)	2.6 (1.7/3.5)	3 (1.6/3.8)	5.6 (4.2/7.6)
ΔP (%)	7.4 (-10.8/36.3)	15.4 (3.1/22.3)	9.9 (-4.1/23.1)	19.5 (-10.3/56.3)
ΔSCA (%)	−10.1 (-17.8/-3.3)	−13.4 (-20/-5.8)	−15.3 (-22.8/-5.6)	−34.8 (-52.3/-24.9)
ΔAET (%)	23.3 (10.6/35.9)	30.6 (18.4/39.4)	30.7 (16.1/41)	52.7 (41.7/72.2)
ΔQ (%)	2.7 (-15.7/32.1)	10.3 (-2.4/17)	2.5 (-12/14.6)	11.7 (-18.6/48.1)
ΔHP Aleo-1 (%)	0	0	0	0
ΔHP Aleo-2 (%)	11.1 (-2.1/28.3)	18.7 (9.8/26.5)	13 (2.2/20.8)	19.7 (-5.4/40.1)

ΔT: absolute change in mean annual temperature; ΔP: relative change in annual precipitation; ΔSCA: relative change in Snow Cover Area; ΔAET: relative change in actual Evapotranspiration; ΔQ: relative change in streamflow at the basin outlet; ΔHP: relative change in annual hydropower generation.

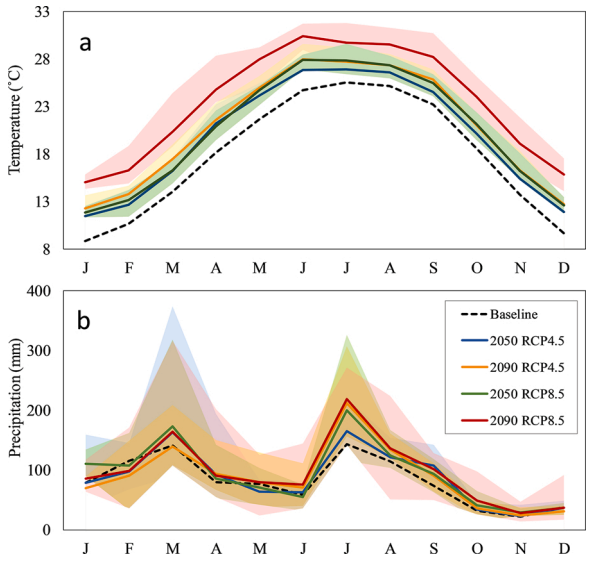

Fig. 4. Monthly means of a) temperature and b) precipitation observed at Bhuntar station for the baseline and the ensemble means of bias corrected outputs of the selected climate models in RCP4.5 and RCP8.5 for the middle and the end of the century. Shading corresponding to the line data denotes the ensemble range of projections within five GCMs.

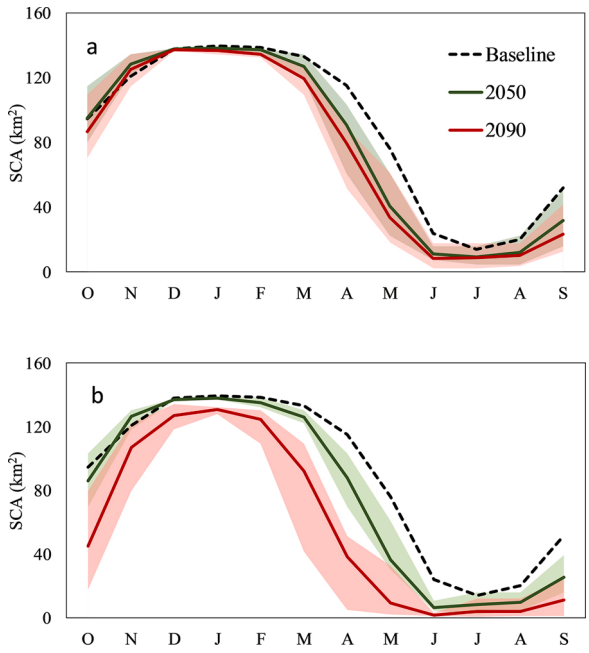

Fig. 5. Simulated mean monthly SCA (km^2) in the catchment till the end of century under a) RCP4.5 and b) RCP8.5. The lines indicate the ensemble mean and the shading denotes the range of WEAP outputs for runs forced with five GCMs projections.

arising from the increase in liquid precipitation in the future (Immerzeel et al., 2012) (Table 5).

The changes in annual river flow also mask important seasonal changes. Simulated winter flows increase by 35.4% (RCP4.5) and 77.8% (RCP8.5) whilst autumn flows increase by 32.6% (RCP4.5) and 48.9% (RCP8.5) by the end of century. Warmer temperatures produce earlier melting of seasonal snow leading to streamflow peaks appearing in May and April in 2050 and 2090, respectively, and the depletion of snow cover, which results in reduced snowmelt that is further reflected in attenuation of summer runoff observed in the dry scenarios. Simulated mean monsoon streamflow is projected to change by -7.2% (RCP4.5) and -12.6% (RCP8.5) by the end of century as the decrease in monsoon flows in dry scenarios overpowers the increase projected by wet scenarios (Fig. 6).

Table 5
Relative contributions of snowmelt, icemelt, rainfall-runoff and baseflow to the annual runoff (%) until the end of the century; the values are the ensemble means of 5 GCM outputs and the values in bracket indicate (minimum/maximum) values.

Period	Snowmelt Runoff	Icemelt Runoff	Rainfall Runoff	Baseflow
Baseline	29.9	3.7	41	25.4
2050 RCP4.5	21.5 (19.1/25.6)	1.20 (1.12/1.44)	49.3 (45.1/51.7)	28 (27.8/28.4)
2050 RCP8.5	20.6 (16.7/25)	1.27 (1.08/1.42)	50 (46/53.6)	28.1 (27.9/28.3)
2090 RCP4.5	16.5 (14.1/18.2)	0	54 (52.3/56.2)	29.5 (29.4/29.8)
2090 RCP8.5	13.8 (10.1/20.6)	0	57 (50.9/60.1)	29.2 (28.5/29.8)

4.4.4. *Future hydropower generation*

The simulated hydropower generation of the Aleo-1 plant is unaffected by the changes in hydrology and cryosphere in the catchment due to the low flow requirement of the plant (Table 4) (Fig. 7). The simulated lowest historical and future flows substantially exceed the flow requirements of the plant. Thus, the hydrological requirement of Aleo-1 is satisfied in all the climate change scenarios, resulting in consistent power generation at maximum productivity throughout the century.

The power production of the Aleo-2 project shows similar behaviour to streamflow; it changes by 2.2 to 20.8% (RCP4.5) and -5.4 to 40.1% (RCP8.5) by the end of the century (Fig. 7). While the wet scenarios show a noticeable increase in hydropower production, dry scenarios show a marginal decrease of 2–5% due to the decrease in the peak generation in monsoon months which is partially offset by increases in the remaining months. The decreasing snowmelt runoff causes the declining trend of simulated power production in June till the end of the century. Simulated power production from October to April continuously increases till 2090 in all the climate change scenarios (Fig. 8), indicating that the Aleo-2 power project is able to take advantage of the increased winter and autumn flows arising from the higher temperature and earlier melting. In the baseline, 10.2 and 10.4% of the total simulated annual hydropower generated

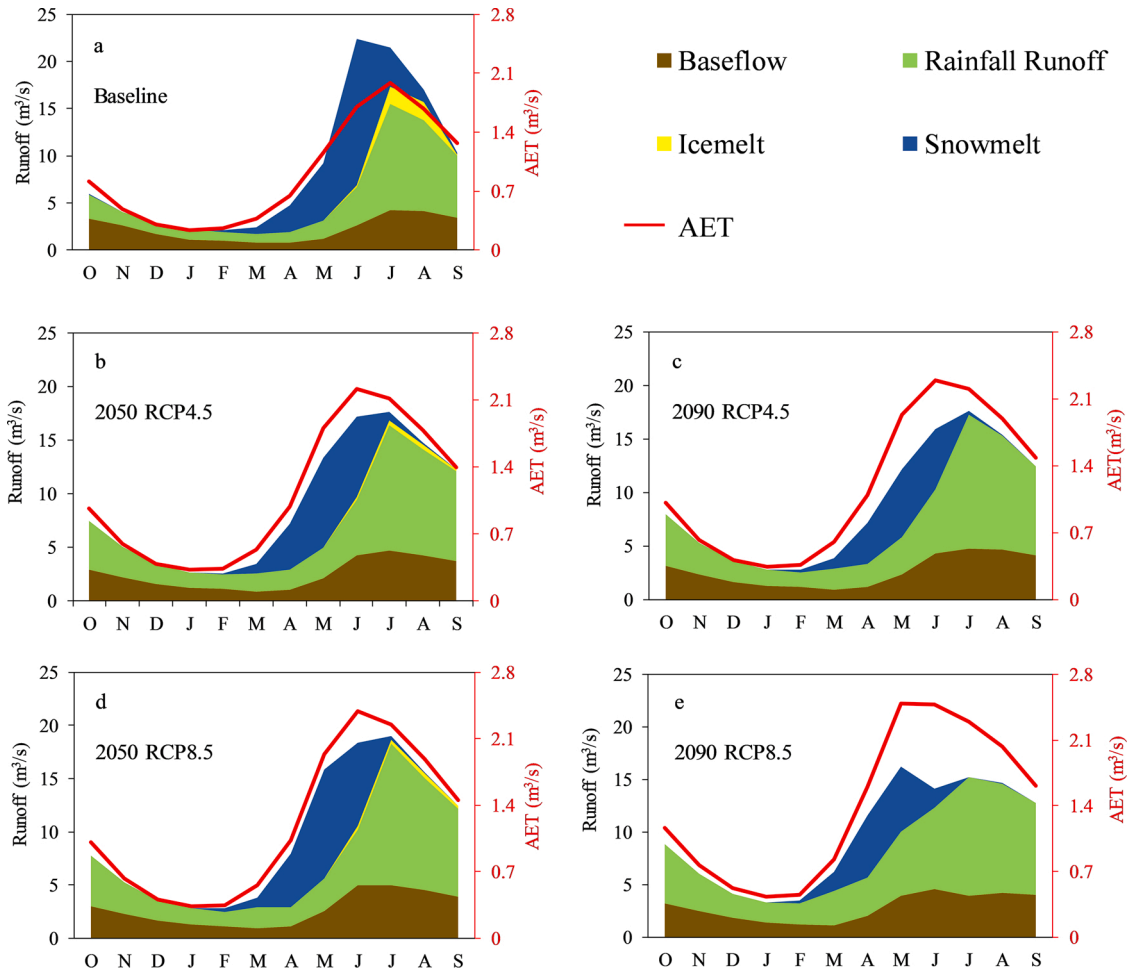

Fig. 6. Mean monthly streamflow components (snowmelt runoff, icemelt runoff, rainfall-runoff and baseflow) and AET until the end of the century for RCP4.5 and 8.5. The values are the ensemble mean of WEAP outputs considering the projections of five GCMs.

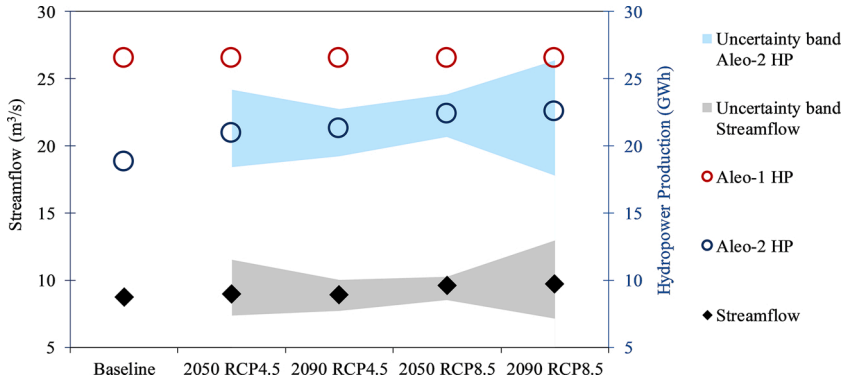

Fig. 7. Projected average annual streamflow (m^3/s) and hydropower production (GWh) at Aleo-1 and Aleo-2 power projects until the end of the century; the values are the ensemble mean and the shading shows the range of WEAP outputs for runs forced with five GCMs projections.

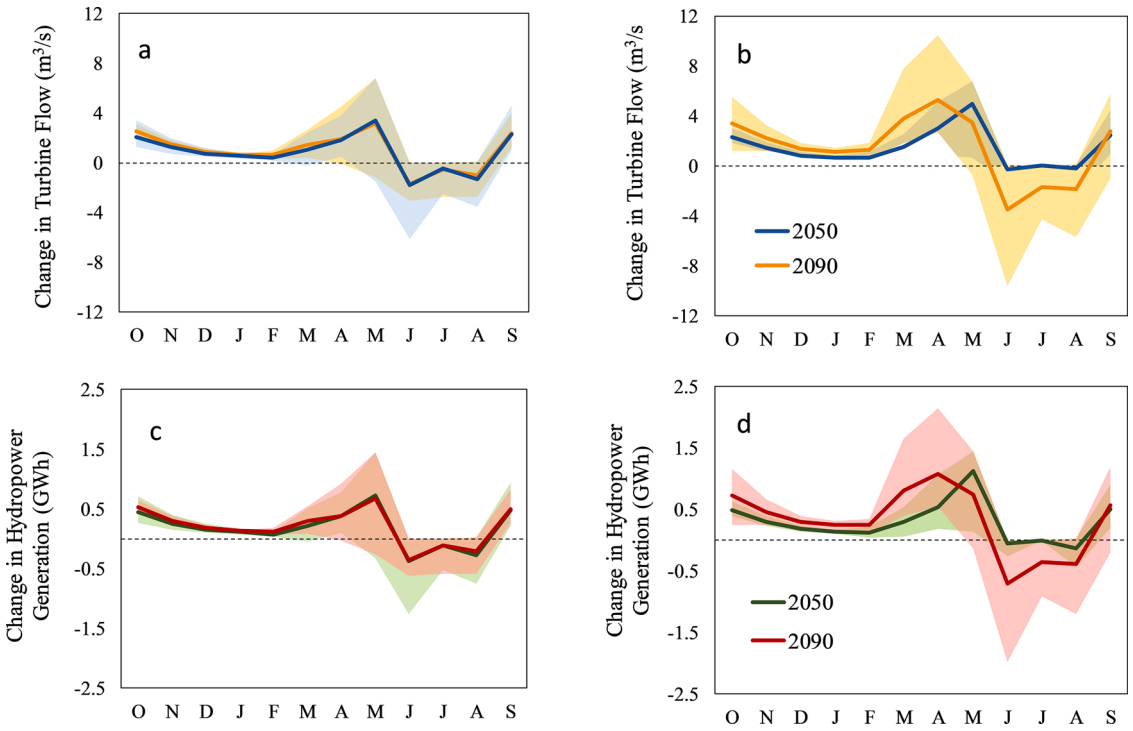

Fig. 8. Panel a and b show changes in mean monthly turbine flow (m^3/s) in RCP4.5 and RCP8.5, respectively. Panel c and d show change in mean monthly hydropower production (GWh) at Aleo-2 power project compared to the baseline for RCP4.5 and RCP8.5, respectively. Lines indicate the ensemble means while the shading indicates the ensemble range of WEAP outputs considering thr projections of five GCMs.

by Aleo-2 is in autumn and winter seasons, respectively. By the end of the century, it increases by 63.7 and 86.3% in RCP8.5, contributing to overall increased power production in wet scenarios and offsetting the decrease in monsoon power production in dry scenarios.

5. Discussions

In the present, snow and glacier melt contribution to the annual runoff is significant (18–44%) which is in agreement with previous studies in the Beas basin (Bookhagen and Burbank, 2010; Kumar et al., 2007; Li et al., 2015, 2019; Momblanch et al., 2019b). Future warmer temperatures lead to increased rainfall runoff contributions at the expense of snowmelt runoff which is further reflected in increases in winter flows by the end of the century. These trends are following the previous studies in the Himalayan catchments (Ali et al., 2018; Immerzeel et al., 2012; Jain et al., 2010; Lutz et al., 2014; Mishra et al., 2020; Momblanch et al., 2019b; Sharma et al., 2013; Su et al., 2016) and imply an increase in water availability in winter. However, the significant decrease in seasonal snowmelt, which is the major contributor of streamflow in pre-monsoon May-June, may reduce water availability for mountain communities. The

findings of this study indicate that while monsoon streamflows show widespread uncertainty depending on the forcing climate, a shift in the seasonality, especially in the increased low flows is prominent in all the climate change scenarios.

Previous studies on the impacts of climate change on hydropower generation in the Himalayan region have either focused on large reservoir hydropower schemes (Ali et al., 2018; Azmat, 2015) or a limited range of small run-of-river hydropower scheme designs (Mishra et al., 2020) in different river basins. Our study is the first to evaluate the impacts of climate change on two highly contrasting SHP designs. In addition, their co-location in the same small catchment means that the simulated differences in climate change sensitivity, as seen in the changing hydropower generation, is solely due to plant design rather than spatio-temporal differences in climate change projections.

Our study has used two ensembles of five GCMs representing a range of possible future climates in the study area which enables us to understand the response of water resources and hydropower plants to a variety of climate change scenarios which largely cover the uncertainty space related to future emissions and climate models. Dry and wet scenarios considered in the study result in the contrasting hydrological impacts of decreased and increased total runoff that can inform understanding of the relative sensitivity of different run-of-river SHP design to future climate change.

Hydropower projects in the Himalayan region which rely on relatively low flows and higher hydraulic heads, such as Aleo-1, provide consistent power generation at maximum productivity throughout the century. They show little sensitivity to the climate change-induced changes in hydrology, as they underutilize available water resources during both the reduced and increased flows of the end-of-century, as indicated by the large amounts of non-power water flows. Their performance is thus robust to the uncertainty in climate change projections. This is consistent with the study of Mishra et al. (2020), who reported that the simulated future changes in inflows across eight GCMs under RCP4.5 and 8.5 to the turn of the century did not translate into significant changes in annual power production at two small power plants in the Karakoram and Central Himalaya, as both mostly operated at their maximum generation limit.

In contrast, SHPs designed for high flows and relatively low water heads, such as Aleo-2, currently work at full capacity in the monsoon season when the streamflow is highest and dramatically reduce generation in winter, as the region is covered in seasonal snow and streamflow is low. Our results show that their future annual and seasonal energy generation are highly sensitive to climate change uncertainty. Under future climate conditions that lead to reduced annual river discharge, as seen in our results of cold-dry and warm-dry scenarios, overall annual energy generation declines slightly but is associated with seasonal generation changes. The increased streamflow in winter and autumn due to increased temperatures and earlier snowmelt allows these power projects to start utilising the increased power potential of low flows (Mishra et al., 2020) that partially offsets the decreased monsoon-season production. However, climate conditions that lead to increased streamflow (as seen in our results of warm-wet and cold-wet scenarios) result in an increase in power production by the end of the century, particularly during the non-monsoon period when energy demand is high.

Overall, low flow hydropower schemes (like Aleo-1) have the benefit of providing a constant and reliable rate of energy generation with negligible sensitivity to climate change uncertainty. However, they are unable to take advantage of increased river flows, and their energy generation does not reflect seasonal energy demands and price variations. High flow schemes (like Aleo-2) have the disadvantage that they provide highly variable (within-year) energy generation and are sensitive to climatic variability throughout the year. However, they can take advantage of the increased hydropower potential in the future, particularly in the non-monsoon period to increase output, enabling energy production to reflect seasonal energy demands and take benefit from seasonal price provisions within power purchase agreements. This study has shown how the design of SHP schemes directly influences their sensitivity to future climate change and the implications for the amount and seasonality of future energy generation. These findings will help reduce the possible impacts of a changing climate on water security and power production and safeguard the investments in the thriving power sector in the mountains through climate-adaptive planning and developments.

6. Conclusions

The present study investigates the impacts of ten climate change scenarios (two ensembles of five GCMs in RCP4.5 and RCP8.5) on water availability and hydropower generation of two contrasting SHP located in the upper Beas basin during 21st century using the WEAP model. The simulated streamflow shows complex relationships between the hydrological response and the future climate with widespread uncertainty in the magnitude and direction. However, significant changes are simulated in the seasonality of streamflow due to rapid changes in the cryospheric components, in particular, leading to earlier snowmelt and a long-term reduction in icemelt. The simulated extent of the catchment's low altitude glaciers in the future decreases rapidly as a response to increasing temperature and disappear entirely by the end of the century. Snow cover area is also projected to decrease continuously following the reducing snowfall.

Hydropower plants with large flow capacity (such as Aleo-2) show a behaviour similar to streamflow projections and are more sensitive to changing climate than SHPs that require low flows but rely on large heads. As more hydropower projects are in the offing in small Himalayan catchments, our study offers insights into possible glacio-hydrological changes and their impacts on power production of alternative SHP plant designs. This understanding can pave the way for climate-adaptive planning and developments of small hydropower projects considering the uncertainty in future climate. It should help the government and the private sector make climate-informed design decisions and assessments of financial risks that will enable SHPs to achieve their potential for supporting energy security, socio-economic development and climate change mitigation in the region.

CRediT authorship contribution statement

Tejal S. Shirsat: Conceptualization, Methodology, Software, Formal analysis, Writing - original draft, Visualization, Writing - review & editing. **Anil V. Kulkarni:** Conceptualization, Investigation, Validation, Resources, Data curation, Supervision, Project administration, Funding acquisition. **Andrea Momblanch:** Investigation, Validation, Writing - review & editing. **S.S. Randhawa:** Data curation, Supervision, Project administration, Funding acquisition. **Ian P. Holman:** Validation, Writing - review & editing.

Declaration of Competing Interest

The authors declare no competing interests

Acknowledgments

The authors would like to thank Divecha Centre for Climate Change (DCCC) at the Indian Institute of Science (IISc) for providing facilities to carry out this research. This research was supported by Science & Engineering Research Board (SERB) of Department of Science and Technology, Government of India, under grant DSTO1952 and UK Natural Environment Research Council grant NE/N015541/1. We are thankful to ADHPL, Manali and Bhakra Beas Management Board for providing in-situ discharge measurements at Allain barrage and meteorological data at Bhuntar station. We also thank Ms. Veena Prasad (DCCC) for the help in future projections of glacier area. Various satellite datasets employed in the study can be accessed from the sources given in the Table 2 in the Section 2. Projections of GCMs were acquired from KNMI Climate Explorer data portal at https://climexp.knmi.nl. Details of the power projects were obtained from the database of UNFCC's Clean Development Mechanism at https://cdm.unfccc.int/Projects/projsearch.html. The authors affirm that no new data was used or generated in the study.

Appendix A. Supplementary data

Supplementary material related to this article can be found, in the online version, at doi:https://doi.org/10.1016/j.ejrh.2021.100797.

References

Ali, S.A., Aadhar, S., Shah, H.L., Mishra, V., 2018. Projected increase in hydropower production in India under climate change. Sci. Rep. https://doi.org/10.1038/s41598-018-30489-4.

Anandhi, A., Frei, A., Pierson, D.C., Schneiderman, E.M., Zion, M.S., Lounsbury, D., Matonse, A.H., 2011. Examination of change factor methodologies for climate change impact assessment. Water Resour. Res. 47, 1–10. https://doi.org/10.1029/2010WR009104.

Azam, M.F., Wagnon, P., Berthier, E., Vincent, C., Fujita, K., Kargel, J.S., 2018. Review of the status and mass changes of Himalayan- Karakoram glaciers. J. Glaciol. 64, 61–74. https://doi.org/10.1017/jog.2017.86.

Azam, M.F., Wagnon, P., Vincent, C., Ramanathan, A.L., Kumar, N., Srivastava, S., Pottakkal, J.G., Chevallier, P., 2019. Snow and ice melt contributions in a highly glacierized catchment of Chhota Shigri Glacier (India) over the last five decades. J. Hydrol. 574, 760–773. https://doi.org/10.1016/j.jhydrol.2019.04.075.

Azmat, M., 2015. Water Resources Availability and Hydropower Production Under Current and Future Climate Scenarios: The Case of Jhelum River Basin, Pakistan. Politecnico di Torino, Porto Institutional Repository. https://doi.org/10.6092/polito/porto/2594956 [Doctoral thesis].

Bolch, T., Kulkarni, A., Kääb, A., Huggel, C., Paul, F., Cogley, J.G., Frey, H., Kargel, J.S., Fujita, K., Scheel, M., Bajracharya, S., Stoffel, M., 2012. The State and fate of himalayan glaciers EH. Science (80-.) 336, 310–314. https://doi.org/10.1126/science.1215828.

Bookhagen, B., Burbank, D.W., 2010. Toward a complete himalayan hydrological budget : spatiotemporal distribution of snowmelt and rainfall and their impact on river discharge. J. Geophys. Res. Earth Surf. 115, 1–25. https://doi.org/10.1029/2009JF001426.

CEA, 2020. Status of Hydro Electric Potential Development, Central Electricity Authority, Government of india. Available from: www.cea.nic.in/reports/monthly/hydro/2019/hydro_potential_region-05.pdf.

Hussain, A., Sarangi, G.K., Pandit, A., Ishaq, S., Mamnun, N., Ahmad, B., Khalid, M., 2019. Hydropower development in the Hindu Kush Himalayan region : issues, policies and opportunities. Renew. Sustain. Energy Rev. 107, 446–461. https://doi.org/10.1016/j.rser.2019.03.010.

Immerzeel, W.W., Van Beek, L.P.H., Konz, M., Shrestha, A.B., Bierkens, M.F.P., 2012. Hydrological response to climate change in a glacierized catchment in the Himalayas. Clim. Change 721–736. https://doi.org/10.1007/s10584-011-0143-4.

Immerzeel, W.W., Lutz, A.F., Andrade, M., Bahl, A., Biemans, H., Bolch, T., Hyde, S., Brumby, S., Davies, B.J., Elmore, A.C., Emmer, A., Feng, M., Fernández, A., Haritashya, U., Kargel, J.S., Koppes, M., Kraaijenbrink, P.D.A., Kulkarni, A.V., Mayewski, P.A., Nepal, S., Pacheco, P., Painter, T.H., Pellicciotti, F., Rajaram, H., Rupper, S., Sinisalo, A., Shrestha, A.B., Viviroli, D., Wada, Y., Xiao, C., Yao, T., Baillie, J.E.M., 2020. Importance and vulnerability of the world's water towers. Nature 577, 364–369. https://doi.org/10.1038/s41586-019-1822-y.

Jain, S.K., Goswami, A., Saraf, A.K., 2010. Assessment of snowmelt runoff using remote sensing and effect of climate change on runoff. Water Resour. Manag. 24, 1763–1777. https://doi.org/10.1007/s11269-009-9523-1.

Kulkarni, A.V., Randhawa, S.S., Rathore, B.P., Bahuguna, I.M., Sood, R.K., 2002. Snow and glacier melt runoff model to estimate hydropower potential. J. Indian Soc. Remote Sens. 30, 221–228. https://doi.org/10.1007/bf03000365.

Kumar, D., Katoch, S.S., 2014. Harnessing 'water tower' into 'power tower': a small hydropower development study from an Indian prefecture in western himalayas. Renew. Sustain. Energy Rev. 39, 87–101. https://doi.org/10.1016/j.rser.2014.07.052.

Kumar, V., Singh, P., Singh, V., 2007. Snow and glacier melt contribution in the beas River at Pandoh Dam, Himachal Pradesh, India. Hydrol. Sci. J. 52, 376–388. https://doi.org/10.1623/hysj.52.2.376.

Li, H., Beldring, S., Xu, C.Y., Huss, M., Melvold, K., Jain, S.K., 2015. Integrating a glacier retreat model into a hydrological model - case studies of three glacierised catchments in Norway and Himalayan region. J. Hydrol. 527, 656–667. https://doi.org/10.1016/j.jhydrol.2015.05.017.

Li, L., Shen, M., Hou, Y., Xu, C.Y., Lutz, A.F., Chen, J., Jain, S.K., Li, J., Chen, H., 2019. Twenty-first-century glacio-hydrological changes in the Himalayan headwater Beas River basin. Hydrol. Earth Syst. Sci. 23, 1483–1503. https://doi.org/10.5194/hess-23-1483-2019.

Lutz, A.F., Immerzeel, W.W., Shrestha, A.B., Bierkens, M.F.P., 2014. Consistent increase in High Asia' s runo due to increasing glacier melt and precipitation. Nat. Clim. Change 1–6. https://doi.org/10.1038/NCLIMATE2237.

Marzeion, B., Jarosch, A.H., Hofer, M., 2012. The cryosphere past and future sea-level change from the surface mass balance of glaciers. Cryosph 1295–1322. https://doi.org/10.5194/tc-6-1295-2012.

Maurer, J.M., Schaefer, J.M., Rupper, S., Corley, A., 2019. Acceleration of ice loss across the Himalayas over the past 40 years. Sci. Adv. 5 https://doi.org/10.1126/sciadv.aav7266.

Maurya, A., Rai, S., Joshi, N., Dutt, K.S., Rai, N., 2018. Snowmelt runoff and groundwater discharge in Himalayan rivers: a case study of the Satluj River, NW India. Environ. Earth Sci. 77, 1–14. https://doi.org/10.1007/s12665-018-7849-9.

Mishra, S., Veselka, T., Prusevich, A., Grogan, D., Lammers, R., Rounce, D., Ali, S., Christian, M., 2020. Differential impact of climate change on the hydropower economics of Two River Basins in High Mountain Asia. Front. Environ. Sci. 8 https://doi.org/10.3389/fenvs.2020.00026.

Momblanch, Andrea, Holman, I.P., Jain, S.K., 2019a. Current practice and recommendations for modelling global change impacts on water resource in the Himalayas. Water (Switzerland) 11. https://doi.org/10.3390/w11061303.

Momblanch, Andrea, Papadimitriou, L., Jain, S.K., Kulkarni, A., Ojha, C.S.P., Adeloye, A.J., Holman, I.P., 2019b. Untangling the water-food-energy-environment nexus for global change adaptation in a complex Himalayan water resource system. Sci. Total Environ. 655, 35–47. https://doi.org/10.1016/j.scitotenv.2018.11.045.

Moriasi, D.N., Arnold, J.G., Van Liew, M.W., Bingner, R.L., Harmel, R.D., Veith, T.L., 2007. Model evaluation guidlines for systematic quantification of accuracy in watershed simulations. Am. Soc. Agric. Biol. Eng. 50, 885–900. https://doi.org/10.1234/590.

Muhammad, S., Thapa, A., 2020. An improved Terra–Aqua MODIS snow cover and randolph glacier inventory 6.0 combined product (MOYDGL06*) for high-mountain Asia between 2002 and 2018. Earth Syst. Sci. Data 12 (1), 345–356.

Mukherjee, K., Bhattacharya, A., Pieczonka, T., Ghosh, S., Bolch, T., 2018. Glacier mass budget and climate reanalysis data indicate a climatic shift around 2000 in Lahaul-Spiti, western Himalaya. Clim. Change 148, 219–233. https://doi.org/10.1007/s10584-018-2185-3.

Negi, H.S., Kanda, N., Shekhar, M.S., Ganju, A., 2018. Recent wintertime climatic variability over the North West Himalayan cryosphere. Curr. Sci. 114.

NEP, 2018. National Electricity Plan, Central Electricity Authority, Government of India. Available from: www.cea.nic.in/reports/committee/nep/nep_%0Ajan_2018.pdf.

Prasad, V., Kulkarni, A.V., Pradeep, S., Pratibha, S., Tawde, S.A., Shirsat, T., Arya, A.R., Orr, A., Bannister, D., 2019. Large losses in glacier area and water availability by the end of twenty-first century under high emission scenario, Satluj basin, Himalaya. Curr. Sci. 116, 1721–1730. https://doi.org/10.18520/cs/v116/i10/1721-1730.

Pritchard, H.D., 2019. Asia's shrinking glaciers protect large populations from drought stress. Nature 569, 649–654. https://doi.org/10.1038/s41586-019-1240-1.

Ragettli, S., Cortés, G., Mcphee, J., Pellicciotti, F., 2014. An evaluation of approaches for modelling hydrological processes in high-elevation, glacierized Andean watersheds. Hydrol. Process. 28, 5674–5695. https://doi.org/10.1002/hyp.10055.

Ragettli, S., Pellicciotti, F., Immerzeel, W.W., Miles, E.S., Petersen, L., Heynen, M., Shea, J.M., Stumm, D., Joshi, S., Shrestha, A., 2015. Unraveling the hydrology of a Himalayan catchment through integration of high resolution in situ data and remote sensing with an advanced simulation model. Adv. Water Resour. 78, 94–111. https://doi.org/10.1016/j.advwatres.2015.01.013.

Rathore, B.P., Kulkarni, A.V., Randhawa, S.S., Bahuguna, I.M., Ajai, 2011. Operationalization of snow & glacier melt runoff model to compute Hydropower potential in Chenab basin, Himachal Pradesh, India. J. Geomatics 5, 53–59.

Sharma, V., Mishra, V.D., Joshi, P.K., 2013. Implications of climate change on streamflow of a snow-fed river system of the Northwest Himalaya. J. Mt. Sci. 10, 574–587. https://doi.org/10.1007/s11629-013-2667-8.

Sieber, J., Purkey, D., 2015. Water Evaluation and Planning System User Guide. Stockholm Environment Institute, Stockholm, Sweden. http://www.weap21.org.

Su, F., Zhang, L., Ou, T., Chen, D., Yao, T., Tong, K., Qi, Y., 2016. Hydrological response to future climate changes for the major upstream river basins in the Tibetan Plateau. Glob. Planet. Change 136, 82–95. https://doi.org/10.1016/j.gloplacha.2015.10.012.

Tahir, A.A., Chevallier, P., Arnaud, Y., Ashraf, M., Bhatti, M.T., 2015. Snow cover trend and hydrological characteristics of the Astore River basin (Western Himalayas) and its comparison to the Hunza basin (Karakoram region). Sci. Total Environ. 505, 748–761.

Tawde, S., Kulkarni, A.V., Bala, G., 2017. An estimate of glacier mass balance for the Chandra basin, Western himalaya, for the period 1984–2012. Ann. Glaciol. 1–11. https://doi.org/10.1017/aog.2017.18.

Tawde, S., Kulkarni, A.V., Govindasamy, B., 2019. An assessment of climate change impacts on glacier mass balance and geometry in the Chandra Basin, Western Himalaya for the 21st century. Environ. Res. Commun. https://doi.org/10.1088/2515-7620/ab1d6d.

Yates, D.N., Sieber, J., Purkey, D.R., Huber-Lee, A., 2005. WEAP21 – a demand-, priority-, and preference-driven water planning model part 1 : model characteristics. Water Int. 30, 487–500 https://doi.org/0250-8060.